Springer Theses

Heteroaromatic Lipoxin A4 Analogues

Synthesis and Biological Evaluation

Bearbeitet von
Colm Duffy

1. Auflage 2012. Buch. xxii, 130 S. Hardcover
ISBN 978 3 642 24631 9
Format (B x L): 15,5 x 23,5 cm
Gewicht: 397 g

Chapter 2
Recent Advances in the Chemistry and Biology of Stable Synthetic Lipoxin Analogues

2.1 Introduction

The Lipoxin metabolites, discussed in Chap. 1, dramatically reduce the bioactivity of this class of compounds and render them poor potential pharmacological agents. In light of the findings associated with the stabilisation and market value of the synthetic prostaglandin and prostacyclin analogues [1], it was thought that a similar approach could be beneficial with respect to the native Lipoxins (LX).

2.2 Design, Synthesis and Biological Evaluation of Stable Lipoxin Analogues

Recent synthetic efforts include mimicking the core structure of the native LXA_4 **1** by replacing certain functionalities with chemically stable motifs with the aim of retaining the potent biological activity. These stable analogues will be sub-divided into three distinct categories (**A**, **B** and **C**), based on the target area being modified, Fig. 2.1. The strategies include (**A**) structural modifications of the $C_{15–20}$ chain: [2] (**B**) replacement of the triene with chemically stable aromatic/heteroaromatic systems: [3, 4] and (**C**) modifications of the $C_{1–8}$ unit [5]. While excellent reviews have extensively covered the synthesis and biological relevance of the native LX and their stereoisomers [6, 7], this chapter will focus on the synthesis and biological evaluation of enzymatically durable analogues.

2.3 (A) Structural Modifications of the $C_{15–20}$ Chain

The desire to prevent oxidation at $C_{15–20}$ led to the design of the first LXA_4 analogues which showed resistance to oxidation [8]. Replacement of this alkyl chain with several different groups furnished a number of analogues with increased pharmacokinetic

C. Duffy, *Heteroaromatic Lipoxin A_4 Analogues*, Springer Theses,
DOI: 10.1007/978-3-642-24632-6_2, © Springer-Verlag Berlin Heidelberg 2012

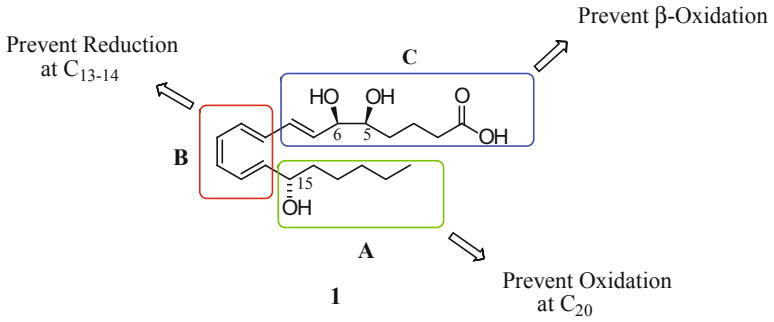

Fig. 2.1 Targeted domains for modifications of the native Lipoxin A_4 **1**

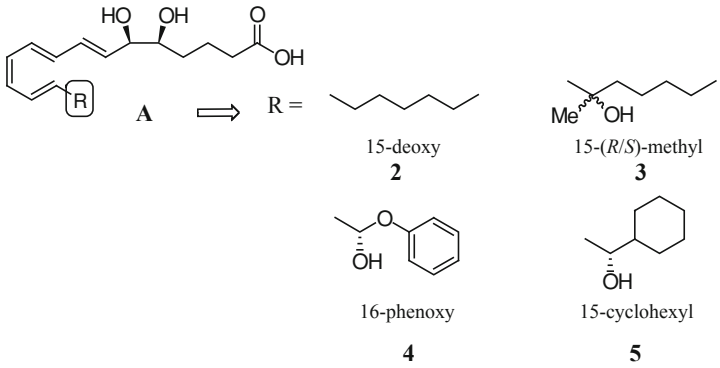

Fig. 2.2 Design of $C_{15–20}$ stable analogues [8]

profiles. Structural adaptations incorporated 15-deoxy-LXA_4 **2**, 15-(*R*/*S*)-methyl **3**, 16-phenoxy **4,** and 15-cyclohexyl **5** into the $C_{15–20}$ chain, Fig. 2.2.

The synthetic routes used for these analogues were not reported in the literature, although they were clearly constructed by using previously reported syntheses for the related native LX [9]. The authors observed that these structural modifications dramatically increased biostability compared to the native LX by preventing dehydrogenation by differential HL-cells and recombinant 15-hydroxyprostaglandin dehydrogenase. The bioactivity was also secured in the 15-(*R*/*S*)-methyl **3**, 16-phenoxy **4** and 15-cyclohexyl **5** analogues due to their ability to prevent PMN transmigration and adhesion in leukocyte migration. The 15-deoxy-LXA_4 **2** showed the least activity suggesting that the hydroxyl group at C_{15} is essential for the preservation of bioactivity.

Alternative analogues have been developed which resulted in enhanced bioactivity compared to the native LX. These designs include the addition of a fluoro **6** and trifluoromethyl **7** group onto the 16-phenoxy analogue **4**, Fig. 2.3 [7, 10].

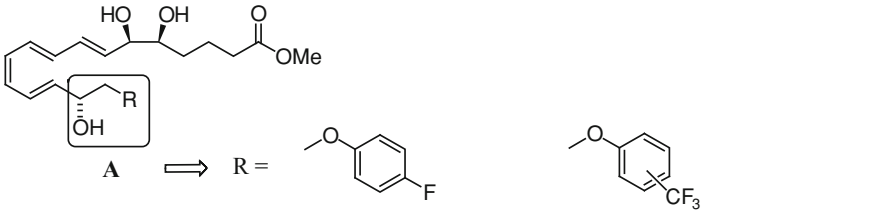

Fig. 2.3 Fluoro and trifluoromethyl stable analogues [7, 10]

The *para*-fluorophenoxy analogue **6** has proven itself to be an extremely potent derivative as it inhibited tumor necrosis factor (TNF)-α-induced leukocyte recruitment into the dorsal air pouch [10]. It was also found to suppress both LTB_4- and PMA-induced recruitment, when applied to mouse ear skin. Furthermore, this analogue has shown potential as an anti-cancer agent, as it inhibits endothelial cell proliferation leading to suppressed angiogenesis at the 1–10 nM range [11]. Realising the potential of these fluorinated analogues, a number of research groups began to develop efficient synthetic routes to these biologically important derivatives. The key synthetic transformations combine a *cis*-reduction of an alkyne, a palladium-catalysed Sonogashira reaction and a Wadsworth–Emmons alkene transformation, Scheme 2.1. Phillips and co-workers reported the first synthesis of the *para*-fluorophenoxy analogue **6** by adopting a chiral pool strategy [2], starting from 2-deoxy-D-ribose **11** [12]. This approach has the advantage of using a readily available starting material which incorporates the two stereocentres which will ultimately appear at C_5 and C_6.

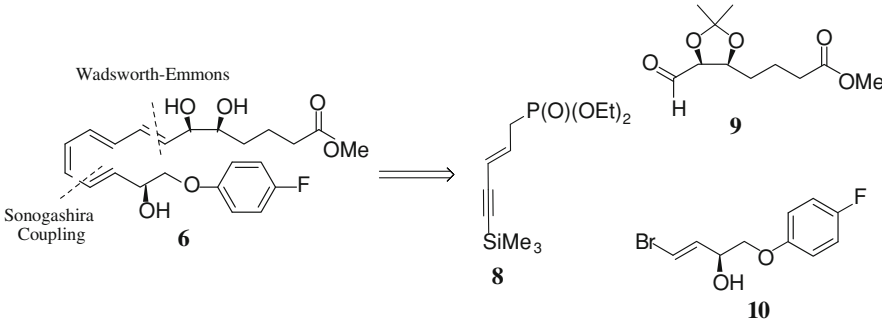

Scheme 2.1 Retrosynthetic analysis of *para*-fluorophenoxy analogue **6**

Protection of 2-deoxy-D-ribose **11** was achieved through its propylidine acetal **12** using 2-methoxypropene and pyridinium *p*-toluenesulfonate (PPTS) in ethyl acetate at room temperature, giving a 43% yield, Scheme 2.2. A Wittig reaction of

methyl(triphenylphosphoranylidine)acetate and the aldehyde form of **12,** followed by a catalytic hydrogenation using 10% Pd/C furnished alcohol **13** in high yields of 81 and 87%, respectively. Oxidation of **13** using Swern conditions afforded aldehyde **9** in 86% yield. This was subjected to a Wadsworth–Emmons transformation with phosphonate **8** and deprotected using KF and 18-crown-6 to form the key intermediate **14** in 99% yield.

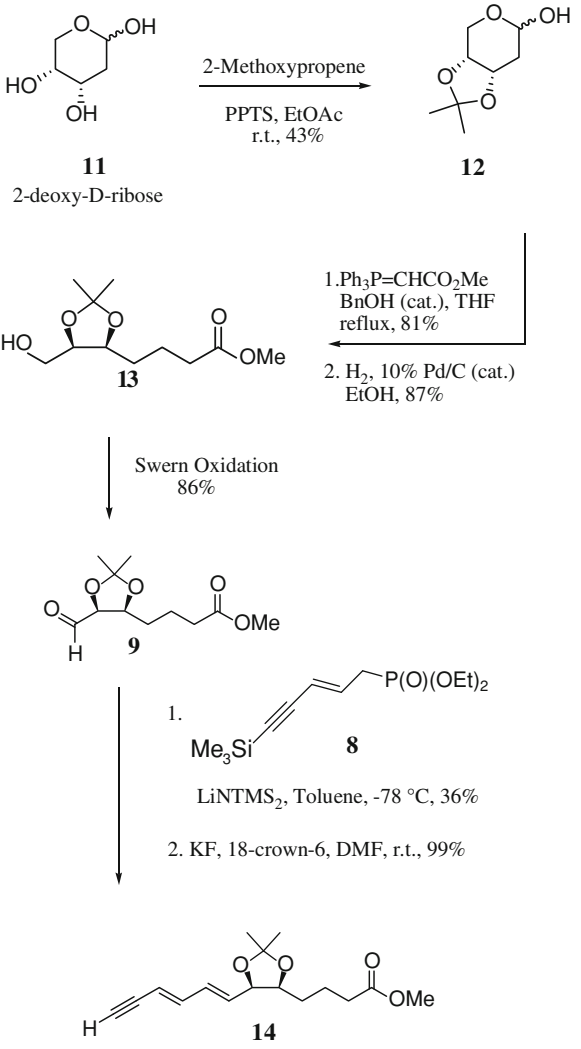

Scheme 2.2 Formation of key intermediate **14** [2]

Phosphonate **8** was itself assembled by the treatment of alkyne **15** with ethylmagnesium chloride and quenching with chlorotrimethylsilane followed by an Appel-type reaction gave the corresponding bromide in 90 and 74% yields,

respectively, Scheme 2.3. This bromide was subjected to Arbusov reaction conditions to afford **8** in 90% yield.

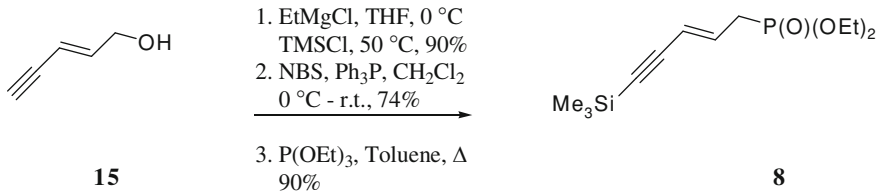

Scheme 2.3 Formation of phosphonate **8** [2]

The synthesis of the Sonogashira coupling partner **10** was accomplished in five steps, beginning with the alkylation of *p*-fluorophenol with 3-chloropropane-1,2-diol **16** in 56% yield, Scheme 2.4. Cleavage of the diol with silica-supported sodium periodate in dichloromethane afforded aldehyde **17** in 98% yield. Addition of lithium 2-trimethylsilylacetylide to **17**, followed by treatment with NaOH to

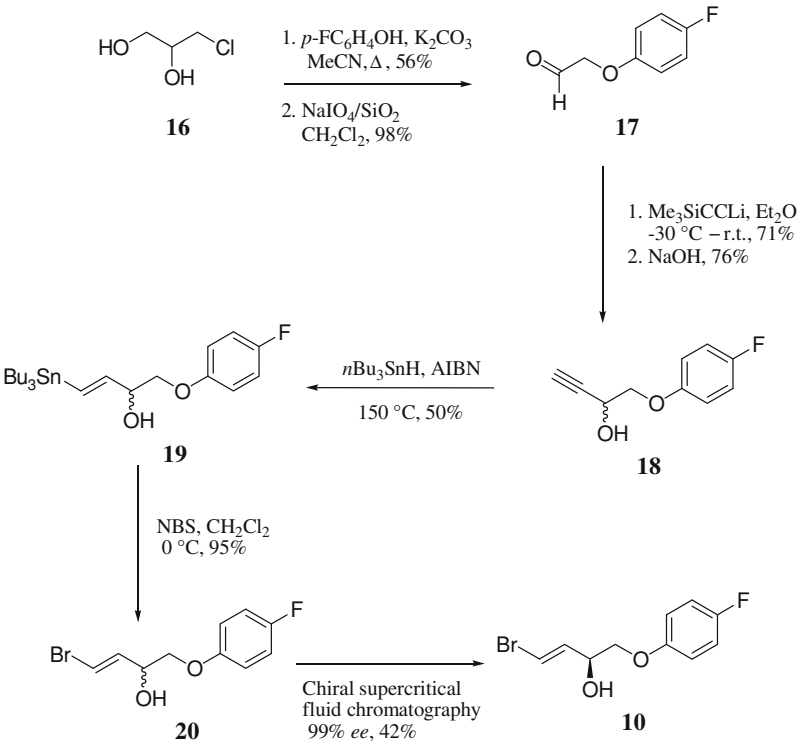

Scheme 2.4 Synthesis of Sonogashira coupling partner **10** [2]

remove the TMS group, gave alkyne **18** in 76% yield. Vinylstannane **19** was constructed by treating **18** with tri-*n*-butyltin hydride. Addition of NBS in dichloromethane to **19** gave the vinylbromide **20** in 95% yield. An attempted kinetic resolution of vinylstannane **19** using Sharpless epoxidation, followed by treatment of the unreacted alcohol with NBS to give **10**, proceeded with poor *ee*. Subsequently racemic **20** was resolved with chiral supercritical fluid chromatography to give vinylbromide **10** in 42% yield and 99% *ee*.

The Sonogashira reaction, employing $Pd(PPh_3)_4$ and CuI in the presence of *n*-propylamine at room temperature, was used to cross-couple vinylbromide **10** and the terminal alkyne **14**, resulting in the formation of **21** in 75% yield, Scheme 2.5. The catalyst loading was not given for this Sonogashira coupling. The acid sensitive acetal group was cleaved by the addition of methanolic HCl to give the corresponding diol. At this stage Lindlar's catalyst can be employed to access the $C_{11–12}$ *cis*-double bond. However, problems have arisen with this method including over-reduction and isomerisation of the $C_{11–12}$ *trans*-double bond isomer during the synthesis of other Lipoxin analogues [13]. Selective *cis*-reduction with an activated zinc alloy has previously been described by Boland [14], and this protocol afforded the *para*-fluorophenoxy Lipoxin analogue **6** in 80% yield. Activation of the zinc requires the addition of 2N HCl for 1–2 min for a clean reaction to take place.

In a similar synthetic approach, starting from 2-deoxy-D-ribose **11**, Petasis and co-workers synthesised stable Lipoxin analogues varying at the $C_{15–20}$ chain, via the introduction of aliphatic, aromatic and fluoroaromatic groups, Scheme 2.6 [7]. The synthetic strategy incorporates a Wittig reaction for the construction of the $C_{7–8}$ double bond, a Sonogashira reaction followed by a *cis*-reduction of the alkyne to establish the $C_{11–12}$ double bond. Simple structural variations of the Sonogashira coupling partners gave rise to many synthetic analogues.

The precise details of the synthesis, including % yields and mol% of catalysts, were not reported as this was part of a review article. The *tert*-butyldimethylsilyl-protected aldehyde **22** was accessed through the chiral pool strategy using 2-deoxy-D-ribose **11**. Compound **23**, previously prepared [13], was reacted with **22** in a Wittig reaction. Double bond isomerisation with I_2 in dichloromethane followed by removal of the trimethylsilyl group by $AgNO_3$ and KCN in EtOH, THF and H_2O gave the alkyne coupling partner **24**. Reaction conditions employed for the Sonogashira reaction included $Pd(PPh_3)_4$, CuI in *n*-propylamine followed by the addition of the corresponding vinyl bromide or iodide. The *tert*-butyldimethylsilyl protecting groups were cleaved using TBAF in THF, followed by reduction of the alkyne, by either H_2 in the presence of Lindlar's catalyst, or by selective *cis*-reduction with an activated zinc alloy, to afford the series of analogues **26**. The 15-cyclohexyl, 15-cyclooctyl and the 16-phenoxy analogues were all found to retain the native Lipoxin bioactions. The inactivation by 15-PDGH and P-450-mediated ω-oxidation were hindered due to the absence of the free ω-alkyl chain. These analogues, of type **26**, were also found be extremely useful in studying the exact binding site in vivo [15]. The fluorinated analogues were found to be the most stable and active in vivo [10].

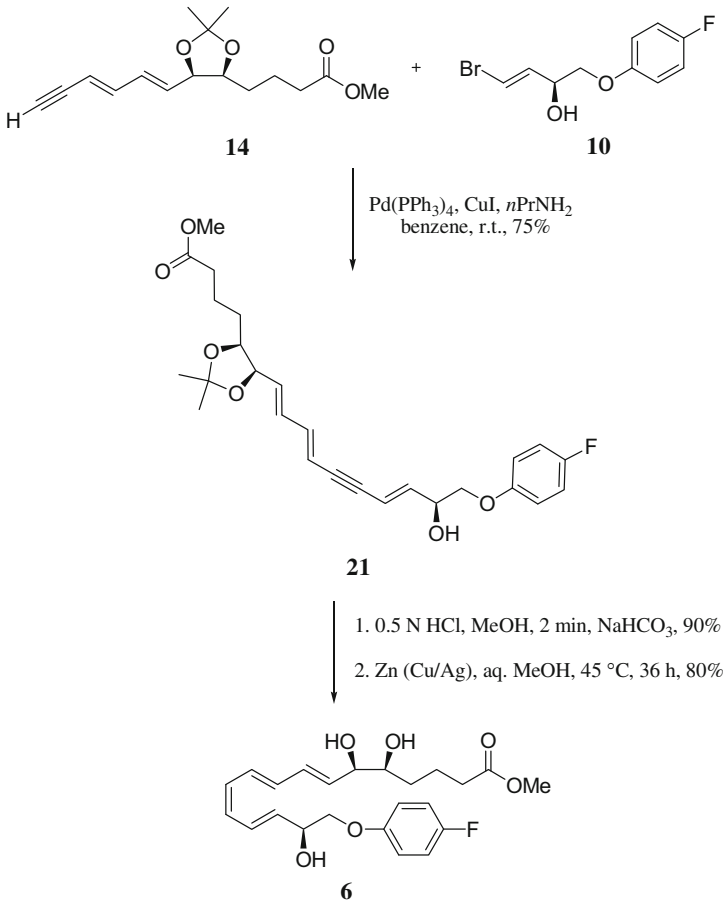

Scheme 2.5 Synthesis of *para*-fluorophenoxy Lipoxin analogue **6** [2]

2.4 (B) Structural Modifications of the Triene

In recent years, researchers have focused their attention on modifying the triene structure of the Lipoxin A_4 and B_4 framework. Derivitisation of this part of the molecule has major advantages in terms of (i) considerably increasing the stability of the molecule towards enzymatic decomposition (ii) development of a short and economical synthesis in an effort to access and screen numerous analogues to further tune the pharmacological profile and (iii) prevention of the double bond isomerisation as described above. Significant advances in the area include the substitution of the triene with aromatic [3, 4] and heteroaromatic rings [16], Fig. 2.4.

The LXA_4 and LXB_4 analogues reported by Guiry and co-workers, **27** and **28** respectively, were constructed using Sharpless asymmetric epoxidation,

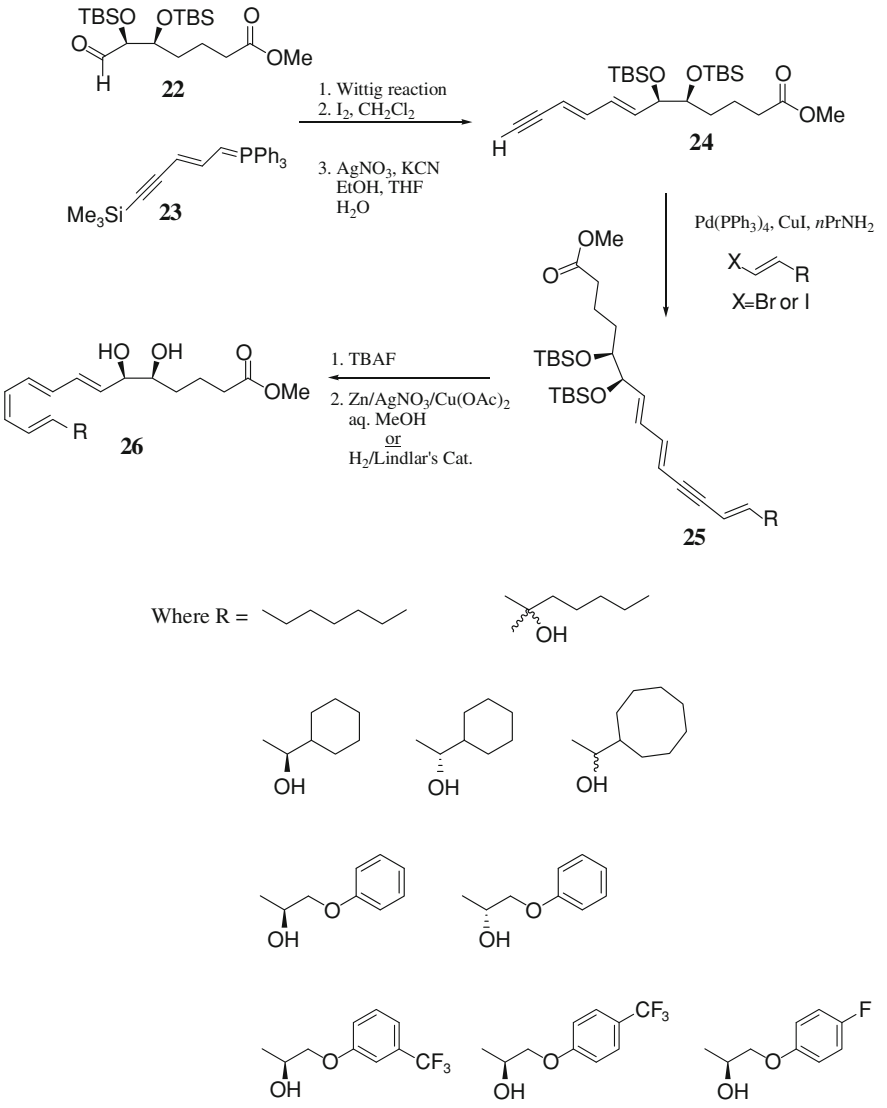

Scheme 2.6 Synthesis of aliphatic, aromatic and fluoroaromatic LXA_4 analogues [7]

Pd-mediated Heck coupling and diastereoselective reduction reactions as the key synthetic transformations [3]. These reactions provided enantio- and diastereoselective generation of each stereocentre and complete control for the formation of the *trans* olefin. In a similar synthetic route Guiry and co-authors synthesised a novel pyridine-containing LXA_4 **29** that was also found to possess important biological properties. The synthesis and biological evaluation of this pyridine-containing LXA_4 **29** will be discussed in detail in Chap. 4.

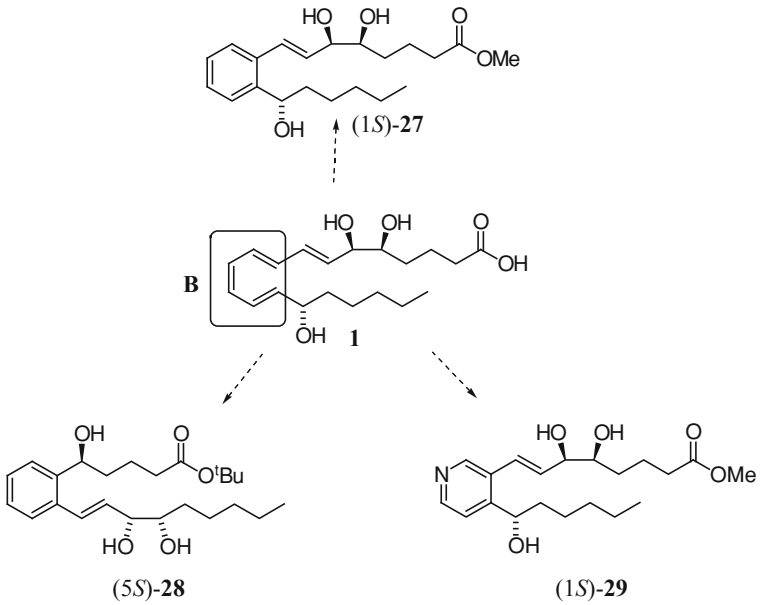

Fig. 2.4 Design of benzene- and pyridine-containing Lipoxin analogues [3]

The first stereoselective route to the novel aromatic analogue **27** described by Guiry and co-workers employed the commercially available divinylcarbinol **30** as the starting material, Scheme 2.7 [3].

This allylic alcohol **30** was subjected to Sharpless asymmetric epoxidation reaction conditions to give the chiral epoxide **31** in 85% yield and with an enantiomeric excess of greater than 99%. Ring opening of **31** with the Grignard derivative of **32** in the presence of a catalytic amount of CuI afforded the desired diol **33** in 82% isolated yield. This diol required an acid stable protecting group as the acidic Jones' reagent was applied to cleave the dioxane in the following transformation. The diol protection was successfully achieved by the addition of acetyl chloride and pyridine in THF at 0°C to give the bisacetate in 97% yield. The addition of Jones' reagent in acetone for 2 h yielded the corresponding acid **34**, which was esterified using diazomethane in diethyl ether. A change of protecting group strategy was employed at this stage as the *bis*-acetate methyl ester was an unsuitable coupling partner for the Heck reaction. For this reason, deprotection with NaOMe in MeOH followed by reprotection with a *tert*-butyldimethylsilyl group was necessary in order to afford the bis-silyl ether **35** in high yield. This protected olefin was then successfully applied in a palladium-mediated Heck reaction in both the benzene- and pyridine-containing LXA_4 analogues, **27** and **29**, respectively. The authors also found that zirconium tetrachloride was an efficient catalyst for a one-pot protection/deprotection synthetic methodology and used this for the synthesis of **35** [17]. This protocol also led to the synthesis of 6-acetoxy-5-hexadecanolide, a component of mosquito oviposition

attractant pheromones [18], and also a microwave-assisted asymmetric synthesis of *exo*- and *endo*-brevicomin [19].

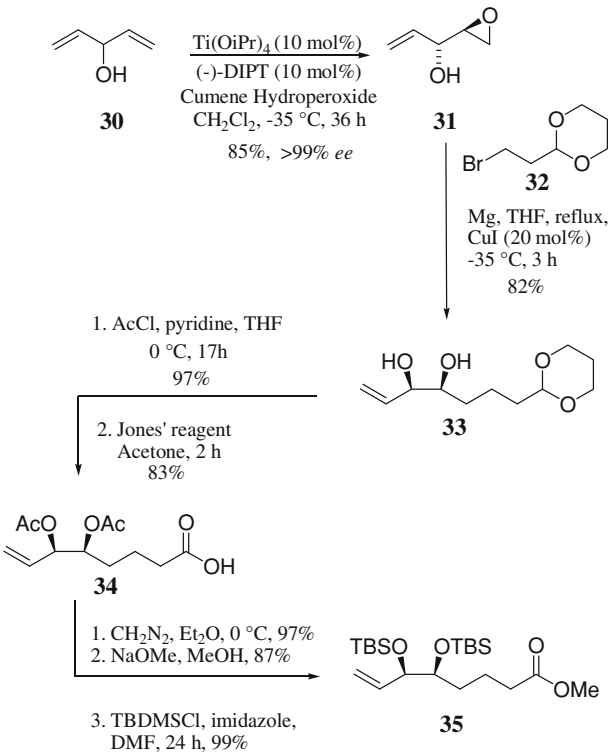

Scheme 2.7 Synthesis of key intermediate **35** [3, 16]

The preparation of aryl bromide **38** required as the other Heck coupling partner was achieved through the addition of the Grignard derivative of 1-brompentane **37** to acid chloride **36**, Scheme 2.8. The reaction was performed at −78°C to prevent any of the double addition product forming. An initial screening of Heck reaction conditions revealed that tributylamine, with its high boiling point, afforded the coupled product **39** in a very high yield (88%). Reduction of this ketone was achieved using sodium borohydride giving rise to a mixture of epimeric alcohols which were easily separated by column chromatography. The authors also employed (–)-*β*-chlorodiisopinocampheylborane to give alcohol **40** in 67% yield and with a 92% diastereomeric excess. Finally this alcohol was deprotected using *p*-toluenesulfonic acid in MeOH giving the triol (1*S*)-**27** in 84% yield. This triol and the (1*R*)-**27** analogue were both converted to their corresponding acids by LiOH in a mixture of methanol and water and were also investigated for their ability to aid in the resolution of inflammation.

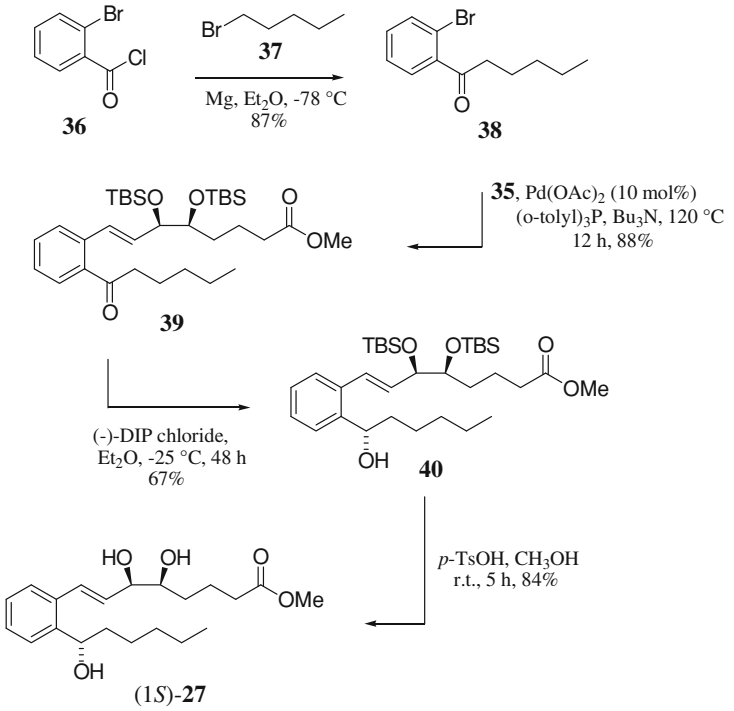

Scheme 2.8 Synthesis of aromatic LXA_4 (1*S*)-**27** [3]

The stereoselective synthesis of the aromatic LXB_4 analogue (5*S*)-**28** exploited a similar synthetic route, assembling the *trans* double via a palladium-catalysed Heck reaction with aryl bromide **43**, Scheme 2.9. The aryl bromide **43**, required for the Heck reaction, was formed through a Sonogashira coupling of 1-bromo-2-iodobenzene **41** and the commercially available terminal alkyne **42**, followed by oxidation with sulfonic acid and esterification.

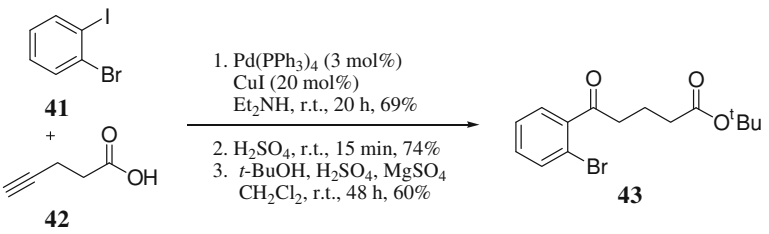

Scheme 2.9 Synthesis of Heck coupling partner **43** [3]

Another epoxide ring opening reaction via Grignard chemistry produced the olefin Heck coupling partner **44**, Scheme 2.10.

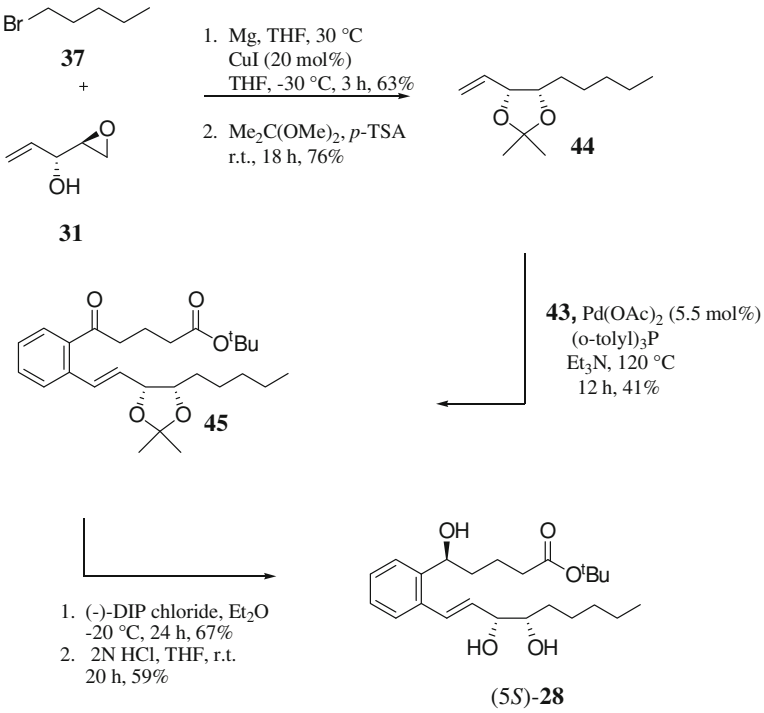

Scheme 2.10 Stereoselective synthesis of aromatic LXB_4 analogue (5*S*)-**28** [3]

The Heck reaction proceeded under similar reaction conditions to those employed for the synthesis of aromatic LXA_4 (1*S*)-**27**, furnishing **45** in 41% yield. Asymmetric reduction of ketone **45** was again accomplished by way of Brown's (–)-*β*-chlorodiisopinocampheylborane to give the alcohol in 67% yield with a de value of 97%. The final step was acetal cleavage using 2N HCl in THF at room temperature to furnish triol (5*S*)-**28** in 59% yield. These new aromatic analogues possess great potential as therapeutic agents as the modular synthetic approach to these compounds renders them extremely accessible and their pharmacodynamics can be further tuned by the addition of known classical bioisosteres.

The novel aromatic LXA_4 analogues (1*S*)-**27** and (1*R*)-**27** promoted increased clearance of apoptotic PMNs when compared to the effect of the native LXA_4, Fig. 2.5.

The aromatic LXB_4 (5*S*)-**28** analogue also stimulated phagocytosis of apoptotic PMNs with a maximum effect observed at 10^{-11} M, Fig. 2.6.

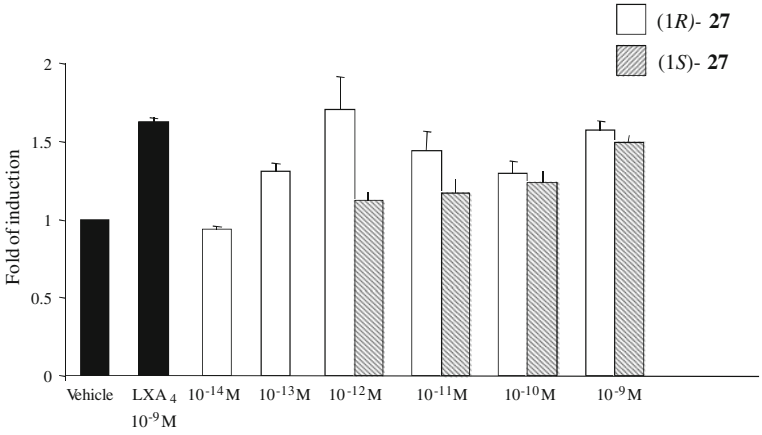

Fig. 2.5 Effect of (1*S*)-**27** and (1*R*)-**27** on the clearance of apoptotic PMNs [3]

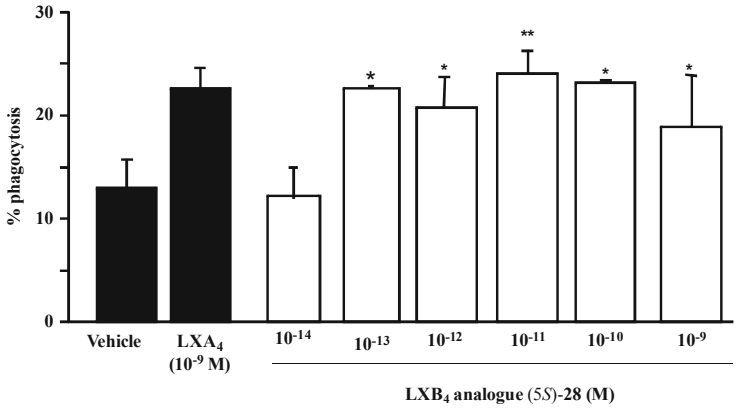

Fig. 2.6 Effect of (5*S*)-**28** on the clearance of apoptotic PMNs [3]

In addition to this, both analogues (**27** and **28**) caused F-actin rearrangement which has also been observed with the native compounds, Fig. 2.7 [20].

Phagocytosis of PMNs was inhibited by pre-treatment with the pan-FPR inhibitor Boc2. This strongly suggests that the effect of these analogues is mediated by the activation of the LX receptor, Fig. 2.8.

These analogues were also screened for their ability to stimulate adherence of monocytes to a matrix such as laminin, Fig. 2.9, which is a previously known property of the native LX and also some of the synthetically stable analogues [21, 22]. In the experiments the acids did not exhibit an increase in phagocytosis over the same concentration range as the methyl esters [3]. This lack of activity

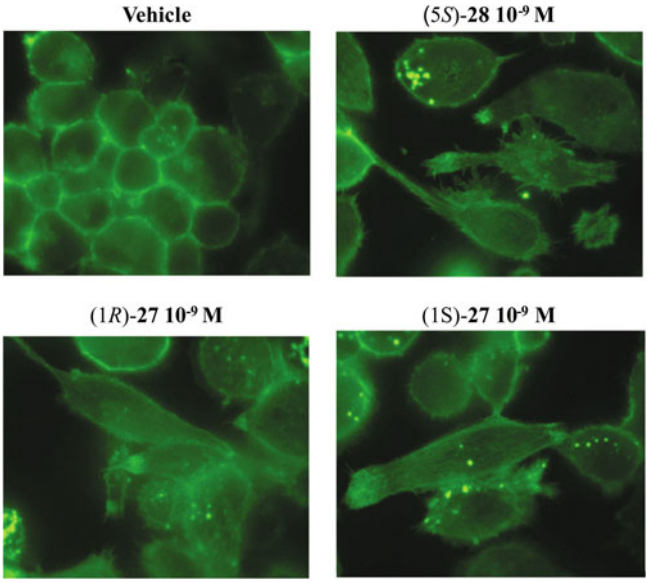

Fig. 2.7 Effect of LX analogues on actin rearrangement inTHP-1 cells [3]

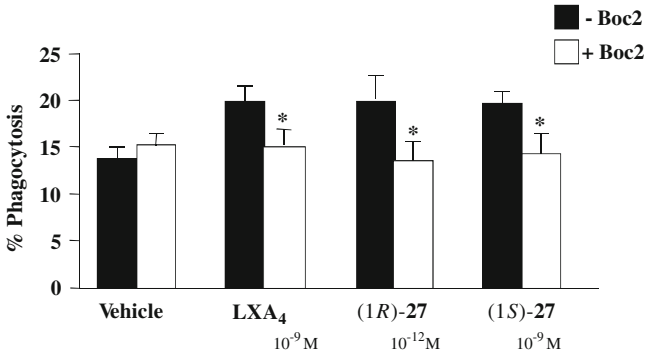

Fig. 2.8 LXA_4 analogues-stimulated phagocytosis of apoptocic PMNs is blocked by the rececptor antagonist BOC2 [3]

was attributed to the fact that the esters act as prodrugs, converting in vivo to the free acid and evoking LX-mediated biological actions [23].

Bannenberg and co-workers also showed that oral administration of LXA_4 has the ability to inhibit leukocyte infiltration in zymosan A-induced peritonitis [24]. Guiry and co-workers found that their (1*R*)-**27** analogue caused a significant decrease in neutrophil accumulation at 50 μg/kg while the (1*S*)-**27** analogue also showed a decrease at the highest dose tested, Fig. 2.10.

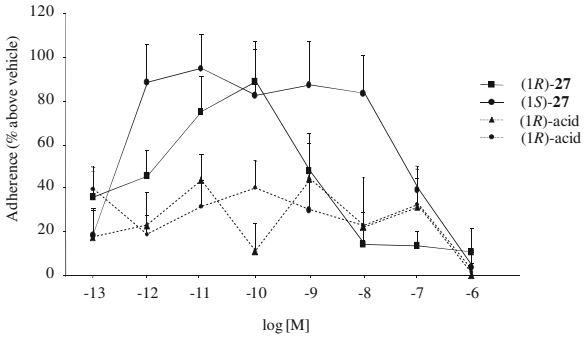

Fig. 2.9 Effect of stable analogues on THP-1 cell adherence to laminin [3]

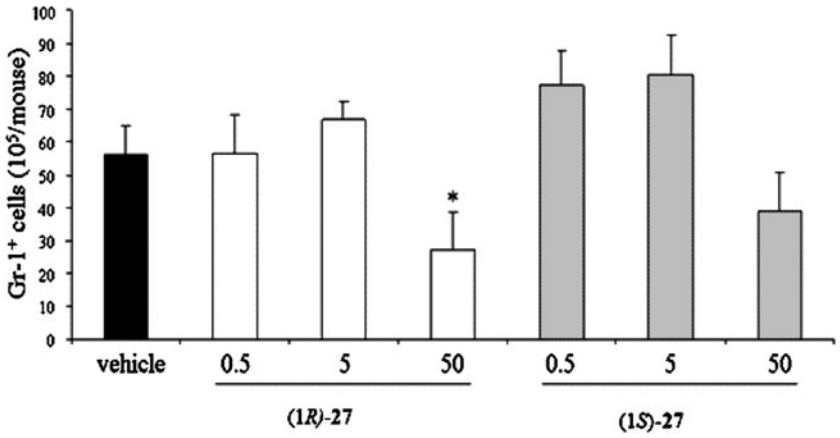

Fig. 2.10 Effect of LXA_4 analogues on zymosan-induced peritonitis [3]

Petasis and colleagues have also successfully managed to stabilise the native LXA_4 **1** with the same approach, replacement of the triene with a more durable benzene ring [4, 25]. Their synthetic route allowed for the synthesis of an array of analogues (**27**, **46**–**49**) Fig. 2.11. Compounds **46**–**49** were designed from a strategy combining domain modifications (**A**) and (**B**), Fig. 2.1.

The synthesis of **46** and **47** relied on two sequential Suzuki–Miyaura coupling reactions, Scheme 2.11. The first combines 2-bromophenylboronic acid **51** and vinyl iodide **50**, which was constructed by a Takai olefination of **22** [13]. Suzuki–Miyaura reaction conditions incorporated $Pd(PPh_3)_4$ and K_2CO_3 using dioxane as the solvent at 60°C furnished **52** in 70% yield. The catalyst loading was not reported in this coupling reaction.

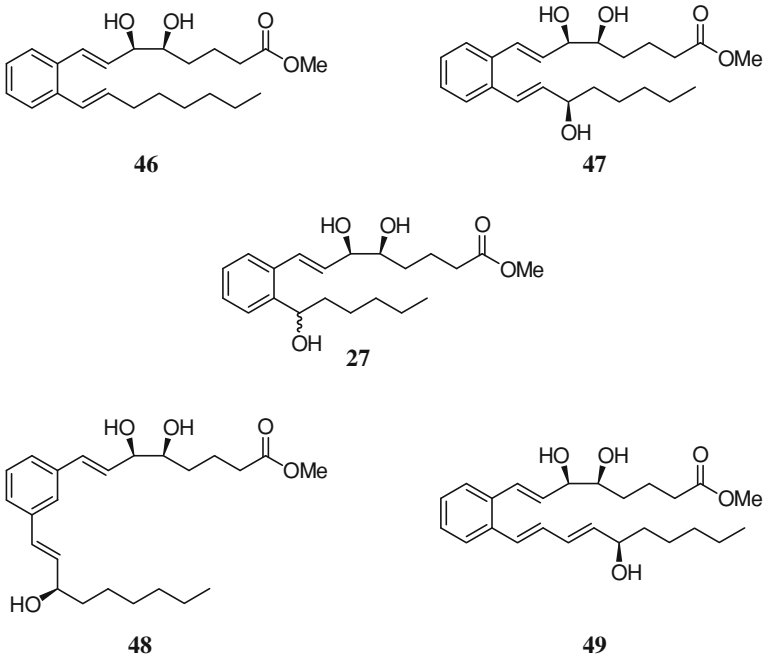

Fig. 2.11 Analogues designed and synthesised by Petasis and co-workers [4]

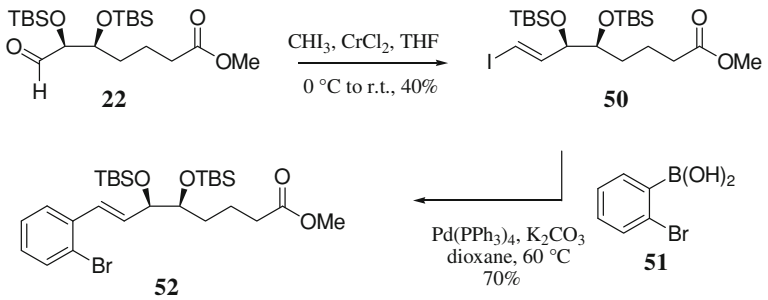

Scheme 2.11 Synthesis of key intermediate **52**

Boronic esters **55** and **56** were both synthesised from the corresponding alkynes **53** and **54**, respectively, Scheme 2.12. Compound **54** was synthesised by the protection of the corresponding alcohol [26, 27].

The second Suzuki–Miyaura coupling combined aryl bromide **52** and boronic esters **55** and **56** in the presence of $Pd(PPh_3)_4$ and K_2CO_3 using a mixure of dioxane and water as the solvent at 80°C, giving **57** and **58** in moderate yields, Scheme 2.13. Deprotection followed with the use of TBAF in THF affording triol **47** and diol **46** in excellent yields.

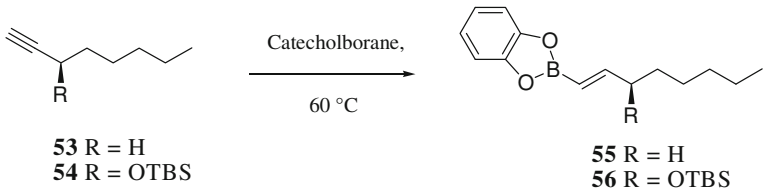

53 R = H
54 R = OTBS

55 R = H
56 R = OTBS

Scheme 2.12 Synthesis of key intermediates **55** and **56** [4]

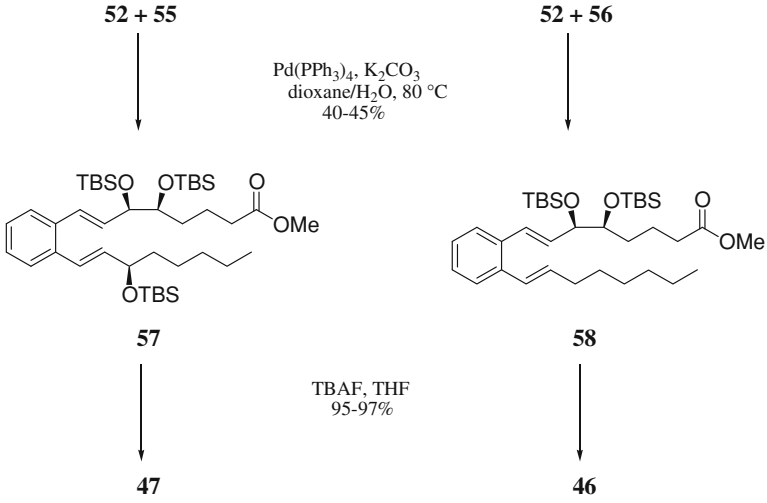

Scheme 2.13 Synthesis of key intermediates **47** and **46** [4]

The same authors also described an interesting and alternative generation of **47** involving a novel and time-conserving one pot boronic acid Heck-type coupling, Scheme 2.14. Both alkenes **35** and **59** were prepared from their corresponding aldehyde precursors, by way of an extremely useful titanium-mediated methylenation developed by Petasis and Bzowej [28]. Firstly, boronic acid **51** reacts with olefin **35** and reactivity is observed solely at the boronic acid position. In the same reaction vessel, a second Heck reaction occurs under reaction conditions reported by Jeffery [29], using $Pd(OAc)_2$, $NaHCO_3$, Bu_4NCl, PPh_3 in acetonitrile at 60°C, giving **57** in 47% yield.

The authors also described the first reported synthesis of a novel *meta*-LXA_4 analogue **48** using a related synthetic pathway starting from 3-bromophenylboronic acid **60**, Scheme 2.15. The vinyl iodide derivative **50** was coupled to **60** by way of a palladium-catalysed Suzuki–Miyaura reaction affording **61** in 70% yield. This aryl bromide **61** was further reacted in a consecutive Suzuki–Miyaura reaction with boronic ester **56**, followed by deprotection with TBAF to give the *meta*-LXA_4 analogue **48** in 42% yield over the final two steps.

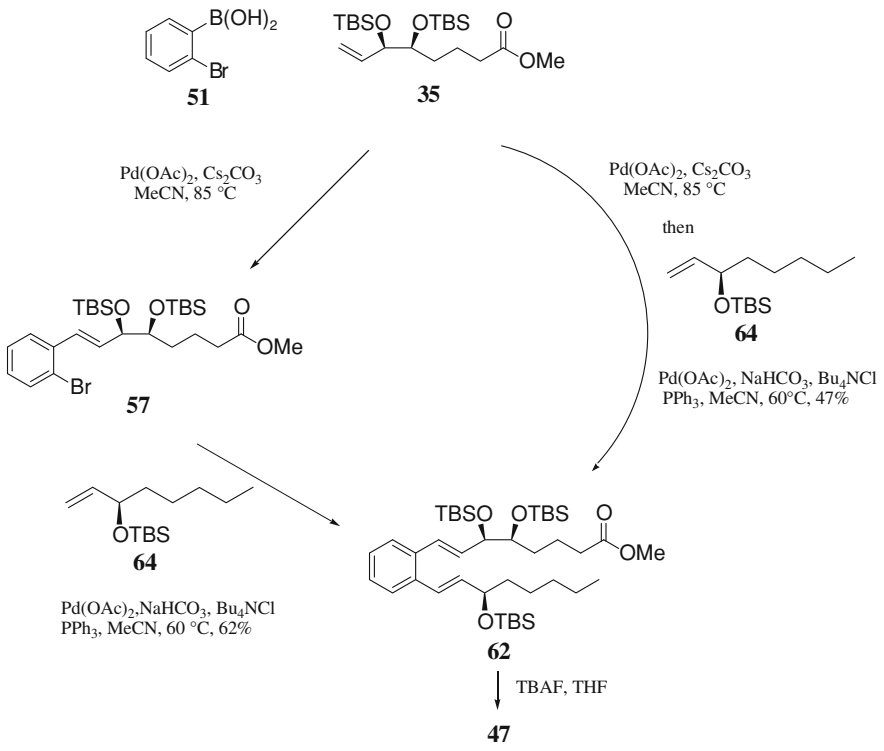

Scheme 2.14 Alternative synthesis of **47** [4]

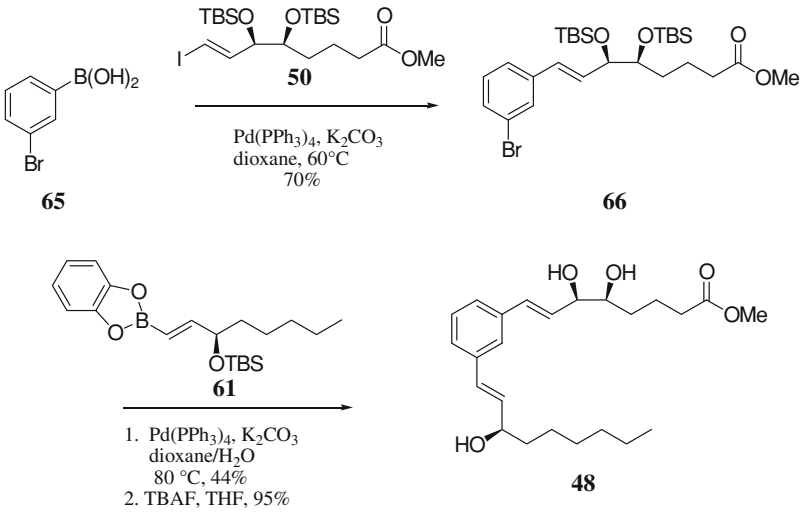

Scheme 2.15 Synthesis of a *meta*-LXA_4 analogue **48** [4]

The LXA_4 analogue **49** was prepared in order to determine the impact of increasing the chain length of the analogues on its ability to act as an agonist in the known receptor site of ALXR. The vinylboronic acid **63** was synthesised by hydroboration of the available 2-bromophenyl alkyne **62**, using the reaction conditions reported by Matteson and co-workers, Scheme 2.16 [30]. The Suzuki–Miyaura reaction of **63** with vinyl bromide **64**, prepared previously [31], gave the aryl bromide **65** in 65% yield. Conversion of this aryl bromide **65** to its pinacol boronate **66** using bis-pinacolato diboron, $PdCl_2$ (dppf) and AcOK in dimethysulfoxide at 80°C proceeded in 40% yield. Boronate **66** was coupled with vinyl iodide **50** by a Suzuki–Miyaura reaction to give the silyl-protected intermediate which was then deprotected to furnish the novel analogue **49** in 43% over the final two steps.

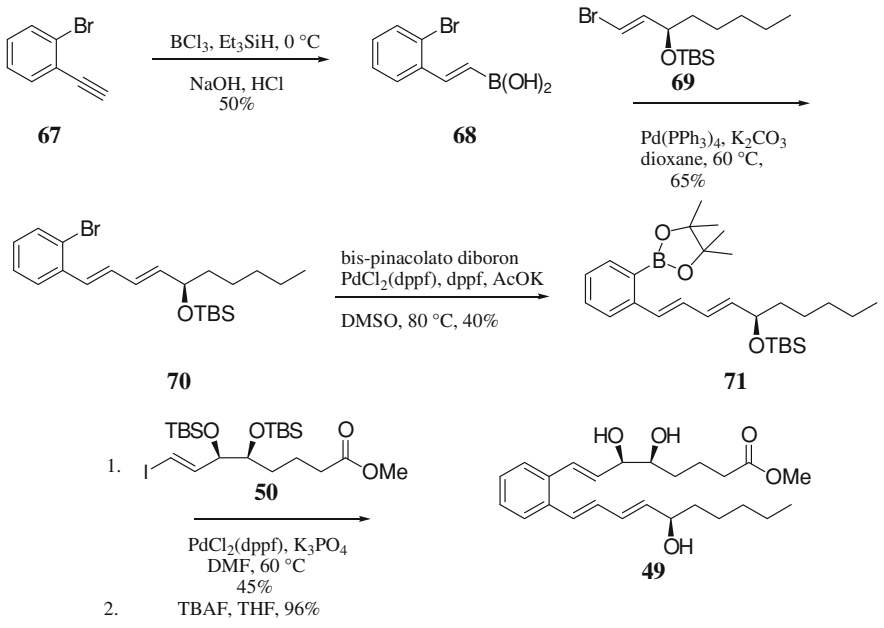

Scheme 2.16 Synthesis of LXA_4 analogue **49** [4]

The same authors also outline a non-stereoselective (at the benzylic position) synthesis of the same benzene-containing LXA_4 **27**, Scheme 2.17, [4] prepared in an asymmetric manner by Guiry and co-workers [3]. The Grignard derivative of bromopentane was prepared and reacted with the Weinreb amide derived from acid chloride **36** to give the aryl ketone in 70% yield. This ketone was then reduced using $NaBH_4$ in MeOH, followed by silyl protection to furnish **67** in high yield. Aryl bromide **67** was converted to its corresponding boronate **68** in a modest 40% yield. The *trans* olefin was constructed by the Suzuki–Miyaura coupling of boronate **68** and vinyl iodide **50** and the epimeric triol **27** was produced in 95% yield after removal of the silyl ethers.

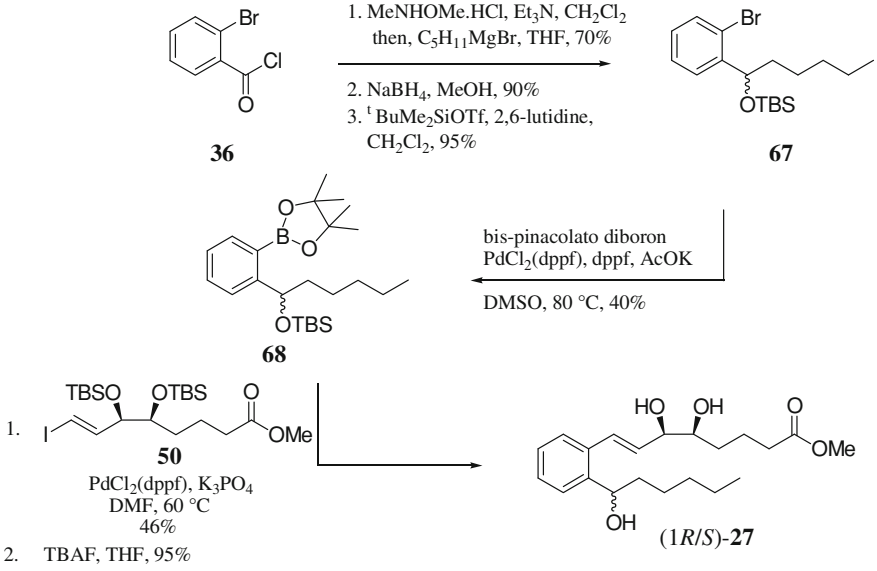

Scheme 2.17 Non-stereoselective synthesis of LXA_4 analogue **27** [4]

Each new stable LXA_4 analogue compiled by Petasis and co-workers (**27**, **46**–**49**) were subjected to enzymatic stability examinations in order to accurately demonstrate their resistance to rapid metabolism by recombinant eicosanoid oxido-reductase (EOR). These compounds were compared to the native LXA_4 **1** to determine which was metabolised the fastest, Fig. 2.12.

The deactivation was monitored by the production of the co-factor NADH. As expected, analogue **46** was the slowest to be metabolised due to the absence of a hydroxyl group on the lower chain.

These new compounds were also tested for their ability to inhibit PMN infiltration by comparison of zymosan A induced-peritonitis in mice, Fig. 2.13.

All of the above new stable analogues were found to be potentially effective anti-inflammatory agents as they increased the inhibition of PMN by up to 32% in the case of **47**. This level of activity is significant as LX and their analogues possess comparable potency to current non-steroidal anti-inflammatory drugs on the market. For example, the anti-inflammatory drug indomethacin **69**, Fig. 2.14, reduces PMN infiltration by 35–40% in the same model of peritonitis [32].

Further to this, the aromatic analogue **47** displayed therapeutic ability to reduce PMN infiltration in murine hind-limb ischemia-induced lung injury, comparable to synthetic analogues that lack the additional benzene ring moiety [24, 25]. Compound **47** was also shown to regulate the production of important cytokines and chemokines known to be fundamental in the inflammatory process [33, 34]. A decrease in MIP-2, TNF-α, and IFN-γ was observed and no effect was observed on the levels of RANTES or SDF-1.

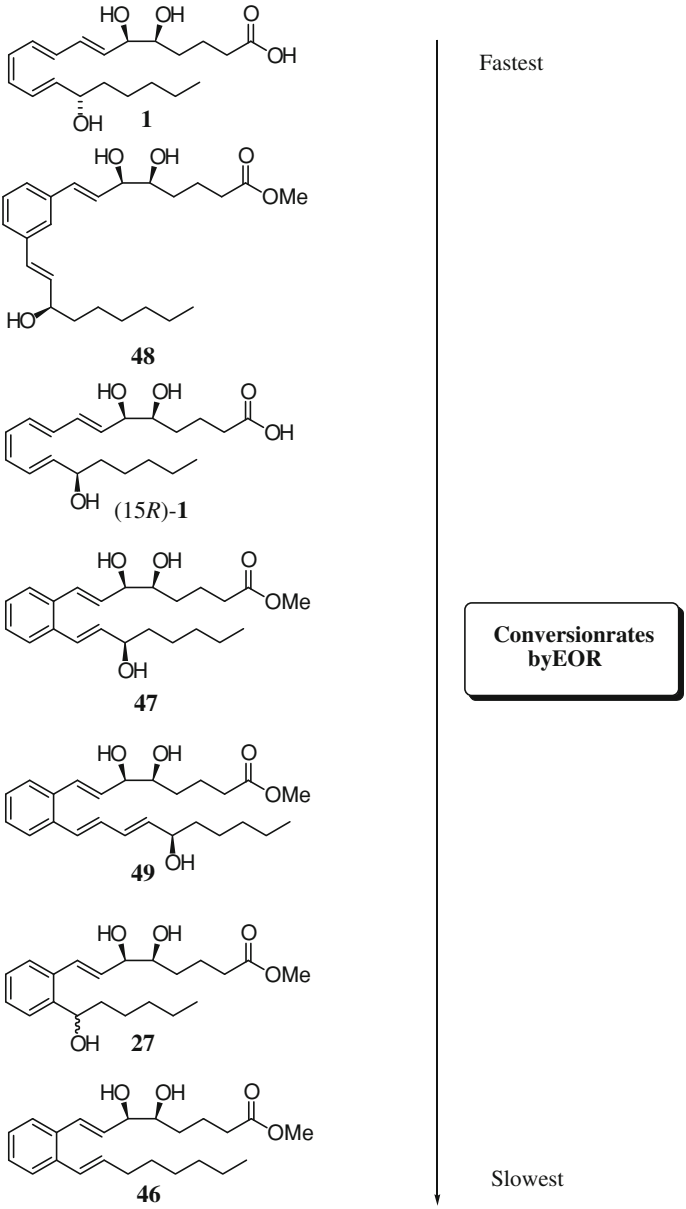

Fig. 2.12 Enzymatic metabolism by eicosanoid oxido-reductase [4]

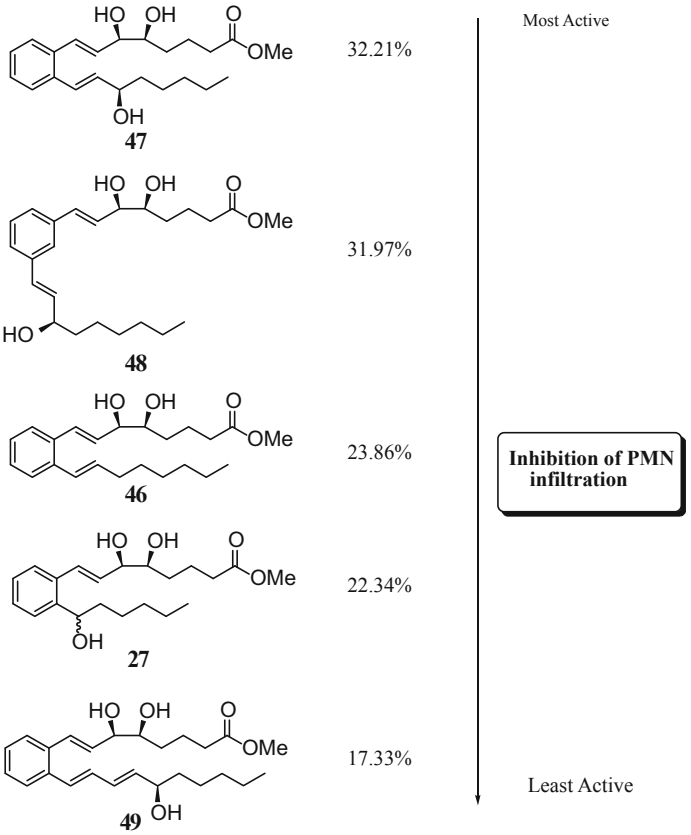

Fig. 2.13 Activity of stable analogues to inhibit PMN infiltration in vivo [4]

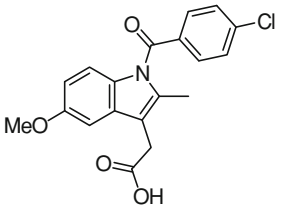

69

Fig. 2.14 Current non-steroidal anti-inflammatory drug indomethacin **69** [32]

2.5 (C) Structural Modifications of the Upper Chain

Although the Lipoxin receptor target has been sequenced [22], the tertiary structure has not been determined to date. Therefore, any extension and/or structural modifications of the upper chains could potentially lead to some attractive

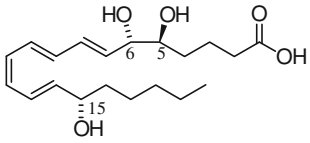

(6*S*)-**1**

Fig. 2.15 Inversion of stereocentre at C_6 [32]

biological findings, as chemical alterations of the lower chain have proven to be extremely advantageous in the previously reported *para*-fluorophenoxy Lipoxin analogue **6**. Structural modification of the top chain is a less researched area as the stereocentres at the hydroxyl groups are essential for bioactivity. The conversion of the stereocentre at C_6 to the corresponding (*S*) stereocentre results in a complete loss of activity, Fig. 2.15 [35].

The C_5 and C_6 hydroxyl groups have displayed resistance to enzymatic metabolism by EOR, therefore rendering this an undesirable part of the Lipoxin structure to alter. However, Guilford and co-workers discovered β-oxidation can occur at C_3 in the *para*-fluorophenoxy analogue **6**, Scheme 2.18 [5].

Stability experiments carried out on plasma samples by Guilford and co-workers revealed an unexpected result. The *para*-fluorophenoxy analogue **6** was converted

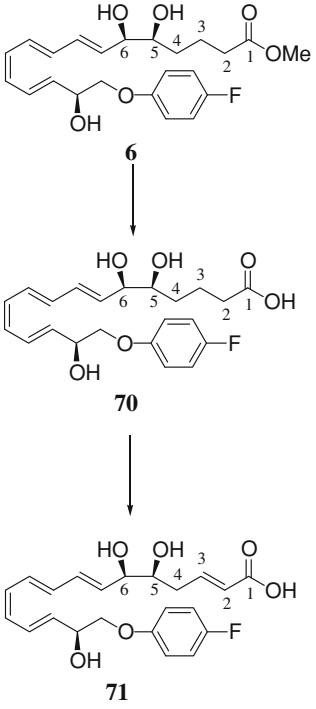

Scheme 2.18 In vivo metabolism of *para*-fluorophenoxy analogue **6** [5]

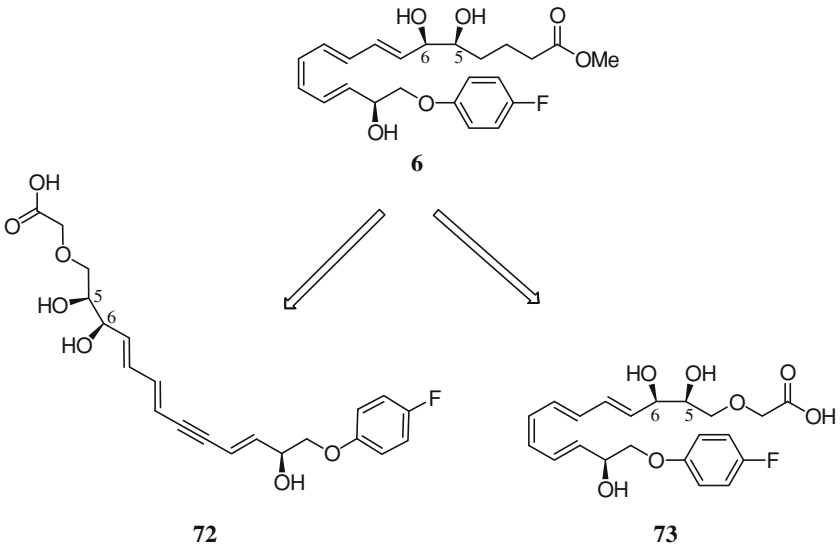

72 **73**

Fig. 2.16 Design of stable analogues **72** and **73** by preventing β-oxidation [5]

into the corresponding acid **70** followed immediately by β-oxidation to furnish the 2,3-dehydro analogue **71**. The assignment of this structure was aided with direct comparisons to the lipid metabolisms of the prostaglandin and the leukotriene pathways previously reported in the literature [36, 37]. With these findings in hand, Guilford designed and synthesised two new LXA_4 analogues (**72** and **73**) by directly replacing the CH_2 group at C_3 with an oxygen to prevent this β-oxidation and hence proposed to enhance the metabolic and chemical stability, Fig. 2.16 [5]. The design of these analogues combines the useful strategy of domain modifications (**C**) and (**A**), Fig. 2.1, modifications the upper and lower chains.

The seleoselective synthesis of **72** and **73** relies upon a Wittig reaction of a known enyne reagent [38], a palladium-catalysed Sonogashira coupling reaction and an activated zinc reduction of an alkyne. A successful chiral pool strategy was utilised in order to achieve the correct stereochemistry at C_5 and C_6 as key intermediates for the Sonogashira coupling reaction were obtained from *L*- Rhamnose **74**, Scheme 2.19.

L-Rhamnose **74** was reacted with sulfuric acid, copper sulfate and cyclohexanone at room temperature for 16 h to afford the corresponding protected cyclohexylidene ketal **75** in 57% yield. This was reduced using $NaBH_4$ in methanol to give the triol **76** in 88% yield. Phase transfer conditions were employed to prepare the required ester which was converted into the corresponding aldehyde **77** in 92% yield using sodium metaperiodate in a mixture of water and acetone. A Wittig coupling of aldehyde **77** and the protected alkyne **78** yielded a 2:1 of mixture of *E,E* and *E,Z* isomers as determined by ^1H NMR spectroscopic analysis. This mixture was dissolved in dichloromethane and treated with iodine to give the required

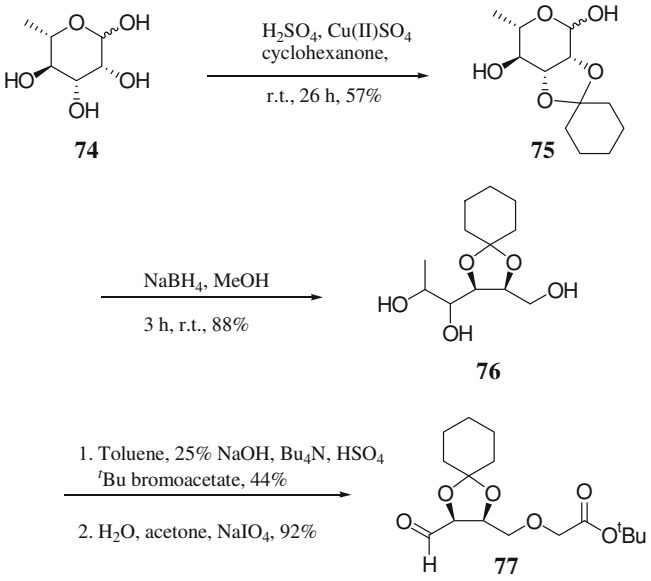

Scheme 2.19 Synthesis of key intermediate **77** [5]

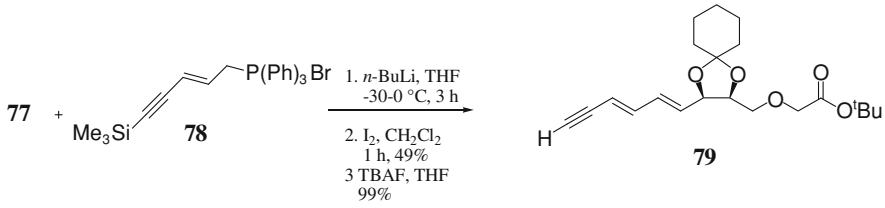

Scheme 2.20 Synthesis of key intermediate **79** [5]

protected *E,E*-dienyne in 49% yield, Scheme 2.20. This was further deprotected using TBAF in THF giving the required terminal alkyne **79** in 99% yield.

The synthesis of the Sonogashira coupling partner **83**, Scheme 2.21, proceeded with the conversion of carboxylic acid **80** into its acid chloride by treatment with oxalyl chloride and a catalytic amount of DMF, followed by direct preparation of the Weinreb amide.

This amide was treated with a solution of ethynylmagnesium bromide to furnish the target ketone **81** in 59% yield over three steps. Ketone **81** was reduced using *R*-Alpine-Borane although with a modest *ee* value of between 60 and 70%. This problem was overcome by the conversion of the alcohol to its dinitrobenzoyl derivative followed by a recrystallization to give *ee* values greater than 98%. This ester was deprotected using K_2CO_3 in MeOH, followed by bromination using NBS

and silver nitrate to form the chiral alcohol **82** in 79% yield over the final two steps. Reduction of the **82** using lithium aluminium hydride and aluminium chloride gave the vinyl bromide **83**, the substrate for a subsequent Sonogashira coupling reaction, Scheme 2.21.

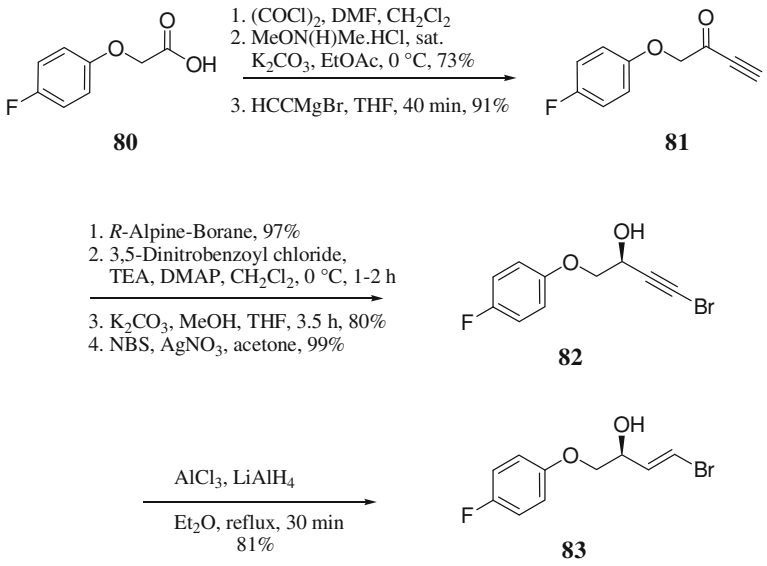

Scheme 2.21 Synthesis of vinyl bromide **83** for Sonogashira coupling

The Sonogashira coupling of **83** and **79** gave the required alkyne in 50% yield, Scheme 2.22. Cleavage of the acetal protecting group with AcOH gave diol **84** in 58% yield. Diol **84** was hydrolysed under basic conditions affording **72** in 58% yield. Reduction using activated zinc, followed by hydrolysis furnished **73** in a low 30% yield.

The natural LX along with stable analogues provide anti-inflammatory benefits in several models of induced skin inflammation [39]. With this information in hand, β-oxidation resistant analogues **72** and **73** were analysed in a calcium ionophore model topically applied to the mouse ear skin. This study revealed comparable potency to the native analogues, by inhibiting edema formation along with a decrease in neutrophil and granulocyte infiltration. Moreover, compounds **72** and **73** have demonstrated the ability to promote the resolution of colitis induced by the hapten trinitrobenzene sulfonic acid which is a model of Crohn's disease [40, 41].

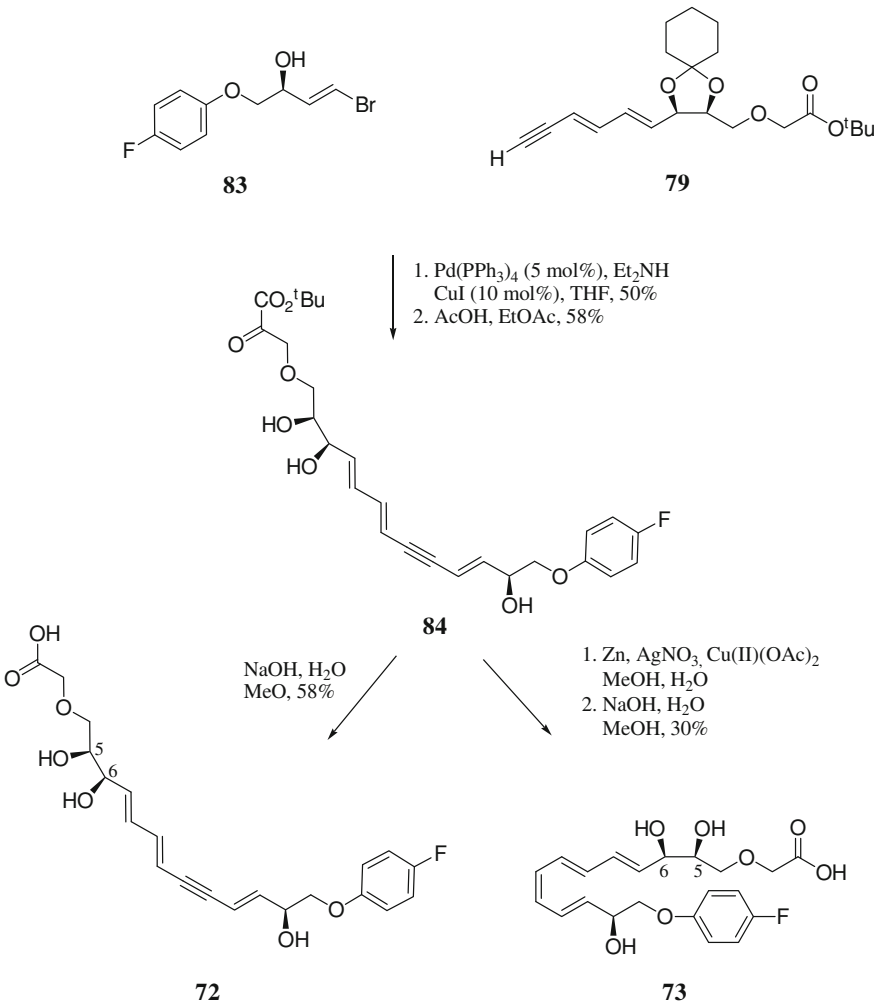

Scheme 2.22 Synthesis of stable analogues **72** and **73** [5]

2.6 Conclusion

Modifications of three key target areas on the LX structure have resulted in the development of Lipoxin analogues displaying increased bioactivity and bioavailability compared to the native LX. The potential biological applications of these stable LX analogues have resulted in a number of efficient synthetic routes being developed for their preparation. Replacement of the $C_{15–20}$ chain by cyclohexyl- and phenoxy-groups and later the further derivatisation of these analogues with fluoro-groups, gave rise to compounds which showed increased biostability and

displayed potential anti-cancer properties. Phillips and Petasis pioneered the research involving stabilisation of this key $C_{15–20}$ chain. Modification of the triene structure which is present in the native LX has been an active area of research. Incorporation of benzene or a heteroaromatic ring in place of this triene structure has had a number of enhanced properties, including stability towards enzymatic decomposition. Guiry and co-workers reported the first stereocontrolled synthesis of a benzene-containing analogue and found that it enhanced the phagocytosis of PMN by macrophages. Guiry and co-workers later published the synthesis of a novel analogue, where the triene had been replaced by a pyridine ring. They found that both epimers displayed potent anti-inflammatory characteristics. There have been fewer reports of structural modifications of the upper chain of the LX, mainly due to the importance of retaining the hydroxyl groups in order to maintain bio-activity. Guilford incorporated oxygen into the upper chain, replacing the β-CH_2 group. This resulted in an analogue that displayed resistance to β-oxidation, leading to heightened metabolic and chemical stability. This derivative also showed potential in the treatment of Crohn's disease.

This chapter reports a concise review of the synthetic and biological developments of novel stable Lipoxin analogues. The major and noteworthy synthetic obstacles and achievements were outlined and discussed. There is an on-going effort to provide novel therapeutic agents to combat an array of inflammatory diseases and it is hoped that this timely review will help to stimulate the design and biological evaluation of novel Lipoxin analogues.

References

1. Collins PW, Djuric SW (1993) Chem Rev 93:1533
2. Phillips ED, Chang H-F, Holmquist CR, McCauley JP (2003) Bioorg Med Chem Lett 13:3223
3. O'Sullivan TP, Vallin KSA, Shah STA, Fakhry J, Maderna P, Scannell M, Sampaio ALF, Perretti M, Godson C, Guiry PJ (2007) J Med Chem 50:5894
4. Petasis NA, Keledjian R, Sun Y-P, Nagulapalli KC, Tjonahen E, Yang R, Serhan CN (2008) Bioorg Med Chem Lett 18:1382
5. Guilford WJ, Bauman JG, Skuballa W, Bauer S, Wei GP, Davey D, Schaefer C, Mallari C, Terkelsen J, Tseng J-L, Shen J, Subramanyam B, Schottelius AJ, Parkinson JF (2004) J Med Chem 47:2157
6. Nicolaou KC, Ramphal JY, Petasis NA, Serhan CN (1991) Angew Chem Int Ed Engl 30:1100
7. Petasis NA, Akritopoulou-Zanze I, Fokin VV, Bernasconi G, Keledjian R, Yang R, Uddin J, Nagulapalli KC, Serhan CN (2005) Prostaglandins Leukot Essent Fat Acids 73:301
8. Serhan CN, Maddox JF, Petasis NA, Akritopoulou-Zanze I, Papayianni A, Brady HR, Colgan SP, Madara JL (1995) Biochemistry 34:14609–14615
9. Webber SE, Veale CA, Nicolaou KC (1988) Adv Exp Med Biol 229:61
10. Clish CB, O'Brien JA, Gronert K, Stahl GL, Petasis NA, Serhan CN (1999) Proc Natl Acad Sci U S A 96:8247
11. Fierro IM, Kutok JL, Serhan CN (2002) J Pharmacol Exp Ther 300:385
12. Rodríguez AR, Spur BW (2001) Tetrahedron Lett 42:6057

13. Nicolaou KC, Veale CA, Webber SE, Katerinopoulos H (1985) J Am Chem Soc 107:7515
14. Boland W, Schroer N, Sieler C, Feigel M (1987) Helv Chim Acta 70:1025
15. Takano T, Fiore S, Maddox JF, Brady HR, Petasis NA, Serhan CN (1997) J Exp Med 185:1693
16. Duffy CD, Maderna P, McCarthy C, Loscher CE, Godson C, Guiry PJ (2010) Chem Med Chem 5:517
17. Singh S, Duffy CD, Shah STA, Guiry PJ (2008) J Org Chem 7:6429
18. Singh S, Guiry PJ (2009) Eur J Org Chem
19. Singh S, Guiry PJ (2009) J Org Chem 74:5758
20. Maderna P, Cottell DC, Berlasconi G, Petasis NA, Brady HR, Godson C (2002) Am J Pathol 160:2275
21. Maddox JF, Serhan CN (1996) J Exp Med 183:137
22. Maddox JF, Hachicha M, Takano T, Petasis NA, Fokin VV, Serhan CN (1997) J Biol Chem 272:6972
23. Chiang N, Serhan C, Dahlén S-E, Drazen JM, Hay DWP, Rovati GN, Shimizu T, Yokomiao T, Brink C (2006) Pharmacol Rev 58:463
24. Bannenberg G, Moussignac R-L, Gronert K, Devchand PR, Schmidt BA, Guilford WJ, Bauman JG, Subramanyam B, Perez HD, Parkinson JF, Serhan CN (2004) Br J Pharmacol 143:43
25. Sun Y-P, Tjonahen E, Keledjian R, Zhu M, Yang R, Recchiuti A, Pillai PS, Petasis NA, Serhan CN (2009) Prostaglandins Leukot Essent Fat Acids 81:357
26. Nicolaou KC, Webber SE (1984) J Am Chem Soc 106:5734
27. Midland MM, McDowell DC, Hatch RL, Tramontano A (1980) J Am Chem Soc 102:867
28. Petasis NA, Bzowej EI (1990) J Am Chem Soc 112:6392
29. Jeffery T (1996) Tetrahedron 52:10113
30. Soundararajan R, Matteson DS (1990) J Org Chem 55:2274
31. Petasis NA, Zavialov IA (1996) Tetrahedron Lett 37:567
32. Hong S, Gronert K, Devchand PR, Moussignac R-L, Serhan CN (2003) J Biol Chem 278:14677
33. Serhan CN, Hong S, Gronert K, Colgan SP, Devchand PR, Mirick G, Moussignac R-L (2002) J Exp Med 196:1025
34. Sodin-Semrl S, Taddeo B, Tseng D, Varga J, Fiore S (2000) J Immunol 164:2660
35. Samuelsson B, Dahlen SE, Lindgren JA, Rouzer CA, Serhan CN (1987) Science 237:1171
36. Ellis CK, Smigel MD, Oates JA, Oelz O, Sweetman BJ (1979) J Biol Chem 254:4152
37. Guindon Y, Delorme D, Lau CK, Zamboni R (1988) J Org Chem 53:267
38. Robinson RA, Clark JS, Holmes AB (1993) J Am Chem Soc 115:10400
39. Schottelius AJ, Giesen C, Asadullah K, Fierro IM, Colgan SP, Bauman J, Guilford W, Perez HD, Parkinson JF (2002) J Immunol 169:7063
40. Fiorucci S, Wallace JL, Mencarelli A, Distrutti E, Rizzo G, Farneti S, Morelli A, Tseng J-L, Suramanyam B, Guilford WJ, Parkinson JF (2004) Proc Natl Acad Sci U S A 101:15736
41. Guilford WJ, Parkinson JF (2005) Prostaglandins Leukot Essent Fat Acids 73:245